RSC Advances

PAPER

View Article Online
View Journal | View Issue

Cite this: *RSC Adv.*, 2023, **13**, 1295

Inconsistent hydrogen bond-mediated vibrational coupling of amide I†

Suranjana Chakrabarty and Anup Ghosh *

Received 12th November 2022
Accepted 16th December 2022

DOI: 10.1039/d2ra07177k

rsc.li/rsc-advances

Using infrared spectroscopy and density functional theory (DFT) calculations, we scrutinized an amide (dimethylformamide) as a "model" compound to interpret the interactions of amide 1 with different phenol derivatives (*para*-chlorophenol (PCP) and *para*-cresol (CP)) as "model guest molecules". We established the involvement of amide I in vibrational coupling with symmetric and asymmetric C=C modes of different phenolic derivatives and how their coupling was dependent upon different guest aromatic phenolic compounds. Interestingly, substitution of phenol perturbed the pattern of vibrational coupling with amide I. The symmetric and asymmetric C=C modes of PC were coupled significantly with amide 1. For PCP, the symmetric C=C mode coupled significantly, but the asymmetric mode coupled negligibly, with amide I. Here, we reveal the nature of vibrational coupling based on the structure of a guest molecule hydrogen-bonded with amide I. Our conclusions could be valuable for depiction of the unusual dynamics of coupled amide-I modes as well as the dependency of vibrational coupling on altered factors.

Introduction

Hydrogen bonds are pervasive in protein molecules, and are involved in biological processes such as molecular association, catalysis, and signal transmission.[1–15] How biologically active, small organic molecules interact with other molecules to elicit different biological effects is an important research area.[16–20] However, identifying the vibrational modes of biologically active molecules (*e.g.*, proteins) is difficult. To overcome such difficulties, the structural and environmental properties of biomolecules have been investigated using "vibrational probes".[21–26]

Many biomolecules contain "amide I", "amide II", "amide III", and "amide A" modes of vibration. However, the amide-I mode is studied widely as a vibrational probe.[27,28] The amide bond is present in many organic molecules and biomolecules.[29–32] Most importantly, as an infrared (IR) probe, amide I is employed extensively because of its sensitivity to the native electric field, solvation, and large molar extinction coefficient.[33–38] In particular, vibrational spectroscopic measurements of the amide-I band are used to monitor shifts in the transition frequency, which is sensitive to the local electric fields as well as interactions with specific "guest molecules".[24–27] Many studies have focused on the relationship between vibrational couplings and conformational dynamics of proteins/peptides.[34–41] Various theoretical methodologies and multidimensional IR-spectroscopy methods have been employed to investigate the vibrational coupling and structural details of biological systems.[42–49] Vibrational coupling and the interactions between different vibrational modes have been investigated.[50] The vibrational coupling between hydrogen bonds associated with amide-A and amide-I/II modes within the same amide component for several dipeptides has been studied using two-dimensional IR spectroscopy.[51] The hydrogen bonding between amide I and phenol derivatives, dimethylformamide (DMF), and dimethyl acetamide has been considered.[52–54]

Investigation of the amide-I vibrational mode is very complex because it is delocalized in biomolecules. However, to study the molecular perceptions and sensitivity of the amide-I mode in the presence of intermolecular hydrogen bonds, we used DMF as a "model" molecule. We measured the IR absorbance of the C=C mode involved in vibrational coupling during intermolecular hydrogen bonding with amide I. Correlations between the hydrogen bond-induced vibrational coupling of C=C and C=O transitions with different factors were investigated by

a, Department of Condensed Matter of Physics and Materials Sciences, S. N. Bose National Centre for Basic Sciences, JD Block, Sector-III, Salt Lake City, Kolkata – 700 106, India. E-mail: anupg86@gmail.com; anup.ghosh@bose.res.in

† Electronic supplementary information (ESI) available: We have provided videos showing coupling of the: symmetric C=C and C=O modes of PC and DMF (AV1); asymmetric C=C and C=O modes of PC and DMF (AV2); symmetric C=C and C=O modes of PCP and DMF (AV3); asymmetric C=C and C=O modes of PCP and DMF (AV4); symmetric C=C and C=O modes of *para*-ethylphenol and DMF (AV5); asymmetric C=C and C=O modes of *para*-ethylphenol and DMF (AV6); symmetric C=C and C=O modes of *para*-nitrophenol and DMF (AV7); asymmetric C=C and C=O modes of *para*-nitrophenol and DMF (AV8); symmetric C=C and C=O modes of *meta*-chlorophenol and DMF (AV9); asymmetric C=C and C=O modes of *meta*-chlorophenol and DMF (AV10); symmetric C=C and C=O modes of *ortho*-chlorophenol and DMF (AV11); asymmetric C=C and C=O modes of *ortho*-chlorophenol and DMF (AV12). See DOI: https://doi.org/10.1039/d2ra07177k

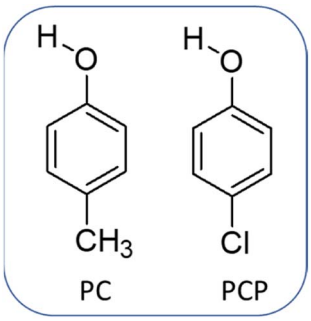

Scheme 1 Chemical structure of the phenol derivatives *para*-cresol (PC) and *para*-chlorophenol (PCP).

employing linear IR spectroscopy. We revealed how pervasive formation of hydrogen bonds in the presence of phenolic compounds (hydrogen-bond contributors) could disturb the amide-I transition and symmetric/asymmetric C=C transition of guest molecules. Hydrogen-bond formation as well as the dependency of vibrational coupling upon different orientations between coupled modes were also investigated in our work.

We employed linear IR spectroscopy and density functional theory (DFT) calculations as theoretical approaches. The frequency gap between symmetric and asymmetric C=C stretching of phenol derivatives and the C=O vibrational mode of DMF, as well as the enhancement factor in IR absorption during vibrational coupling, were monitored in the presence of different donor molecules. Vibrational coupling in biomolecules is important to understand the many biological interactions and processes at the microscopic level, so the coupling of amide I must be investigated. Overall, this structural evidence of vibrational coupling can be used to elucidate many biological and chemical effects.

Experimental section

Para-chlorophenol (PCP; 99.9% purity), *para*-cresol (PC; 99.9% purity), and DMF (99.9% purity) were purchased from MilliporeSigma and used without additional purification. The chemical structure of PCP and PC are drawn in Scheme 1. A solution of DMF (0.1 M) in carbon tetrachloride (CCl_4) was used for linear IR spectroscopy. The sample was placed in a home-made Fourier transform infrared (FTIR) sample cell with CaF_2 windows and a Teflon™ spacer (60 μm). Linear IR absorption spectroscopy was undertaken using an FTIR spectrometer (JASCO-FTIR-6300). The background of the solvent (CCl_4) was measured and subtracted from all spectra of interactions between DMF and phenol derivatives. The Beer–Lambert law was validated by plotting the area of IR absorbance for the C=C mode *vs.* concentration (Fig. S1, ESI†).

Theoretical section

We wished to gain detailed knowledge about the IR absorption spectra of the C=O mode in DMF and C=C mode of different phenol substitutions, so we undertook DFT calculations employing Gaussian 09. In a preliminary manner, all the initial geometries of DMF and different phenolic complexes were optimized by the B3LYP/6-311G+ (D, P) level of theory. Then, calculations to determine the frequency of IR absorption were done for all DMF–phenol hydrogen-bonded complexes.

Results and discussion

A series of linear IR spectra of DMF solution (0.1 M) in CCl_4 were taken with increasing concentrations of PC and PCP from 0 M to 0.05 M (Fig. 1). Preliminarily, the IR absorption frequency of the C=O mode was shown to be 1686 cm^{-1} (black single peak) in the absence of phenolic compounds (0.00 M). With gradual addition of PC or PCP, the IR absorbance of amide 1 decreased progressively and the frequency shifted towards a lower-wavenumber region (Fig. 1a and b, respectively). Fig. 1 reveals that increasing the concentration of PC and PCP led to hydrogen-bond formation of C=O and gradual shifting of the peak position of IR absorption. However, in PC (0.1 M) and PCP (0.1 M), with a gradual increase in the DMF concentration, the IR absorption spectra for symmetric and asymmetric C=C modes showed anomalous behaviours (Fig. 2). For PC, the IR

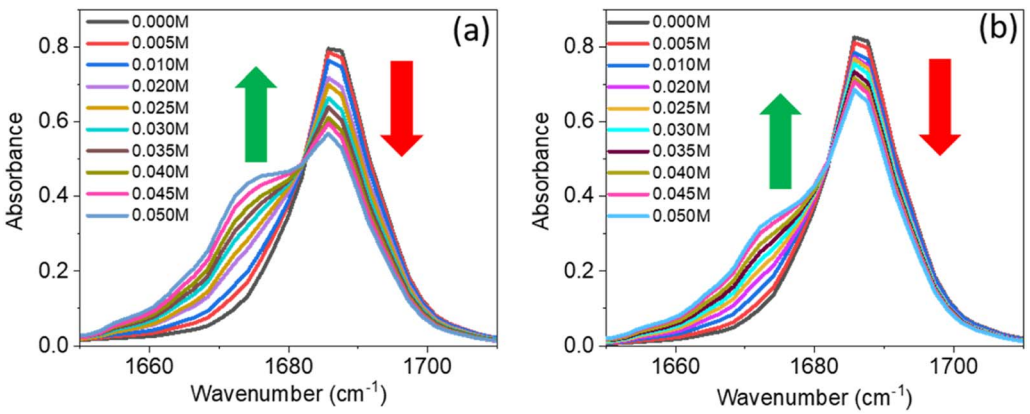

Fig. 1 Linear IR spectra of amide I (dimethylformamide) in the presence of different concentrations of (a) *para*-cresol and (b) *para*-chlorophenol. The colour of the spectra is described in the inset with different concentrations of *para*-cresol and *para*-chlorophenol. The green (up) and red arrow (down) represent enhancement and suppression of absorbance, respectively.

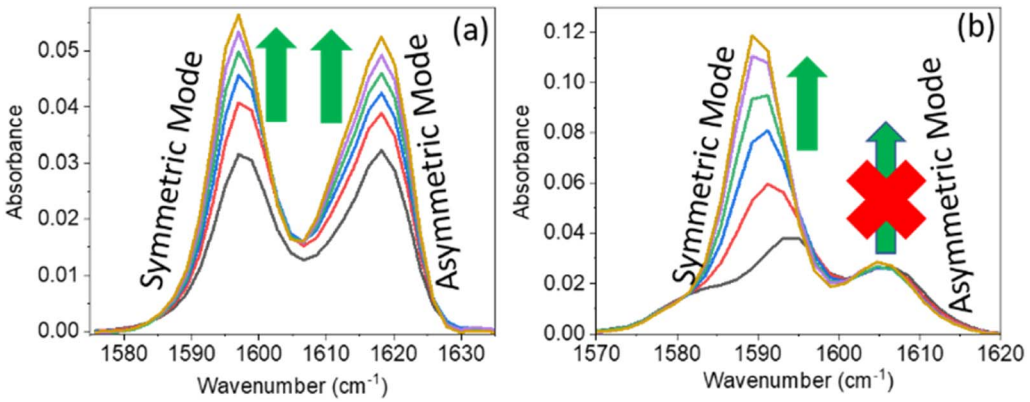

Fig. 2 Linear IR absorption of the C=C mode of (a) *para*-cresol (0.1 M) and (b) *para*-chlorophenol (0.1 M) in the presence of dimethylformamide at 0.00 M (black), 0.02 M (red), 0.04 M (blue), 0.06 M (green), 0.08 M (violet), and 0.10 M (dark-yellow). The green arrow represents enhancement of absorbance. The red cross represents no enhancement of absorbance.

absorption peaks for symmetric and asymmetric C=C modes were at 1597.5 cm^{-1} and 1618.5 cm^{-1} (Fig. 2a) whereas, for PCP they were at 1594.0 cm^{-1} and 1606.5 cm^{-1}, respectively (Fig. 2b). For PC and PCP, with an increasing concentration of DMF (0.000–0.10 M), a significant difference in IR absorbance was observed between symmetric and asymmetric C=C modes (Fig. 2). For PC, with a gradual increase in the DMF concentration from 0.000 M to 0.10 M, IR absorbance for symmetric and asymmetric C=C modes was enhanced significantly. However, in contrast with PCP, though IR absorbance for symmetric C=C stretching was enhanced, IR absorbance for asymmetric C=C stretching was altered negligibly throughout the experiment (Fig. 2). The IR-absorbance enhancement ratio for the symmetric and asymmetric C=C modes of PC was 1.35 and 1.40 whereas, for PCP, it was 5.97 and 1.00, respectively (Table 1), as calculated from Fig. 2. The transition dipole moment of the symmetric and asymmetric modes of PC and PCP changed accordingly (Table 1). These unusual phenomena focused our attention on the intermolecular interactions between amide (C=O) and phenolic compounds (PC and PCP).

The increase in IR absorbance of the C=C mode could have been due to the altered hydrogen bonding with vibrational modes or n–π* bonding of PC and the PCP ring with the C=O mode of DMF (Fig. 2a and b). To elucidate the precise reason underpinning the enhancement, we undertook IR spectroscopy of a 1 : 1 DMF : anisole mixture. The unaltered enhancement of IR absorbance for the C=C mode of the DMF : anisole (1 : 1) mixture signified no interaction of the non-bonded electron of the oxygen atom of DMF with the π electron cloud of anisole. We did not know whether the enhancement was due to the altered electron density of the phenolic ring (C=C mode) after hydrogen bonding with DMF, so we undertook IR spectroscopy of a mixture of acetonitrile (ACN) and phenol at a ratio of 1 : 1 (Fig. 3b). The shifting to a higher IR absorbance frequency of CN signified formation of a hydrogen bond between ACN with phenolic OH (Fig. 3b). An absence of enrichment of IR absorbance of C=C explained the non-involvement of hydrogen bonds. Hence, these results suggested that the enhancement in IR absorbance of the C=C mode was not due to n–π* bonding or hydrogen bonding. Therefore, the enhancement was probably due to vibrational coupling between the C=C and C=O modes of amide (DMF) and phenol derivatives (PC and PCP).

To check that our hypotheses on vibrational coupling were robust, we carried out DFT calculations (b3lyp, 6311 G (d, p)) for PC and PCP hydrogen-bonded with DMF, and the videos are provided in ESI† (AV1, AV2, AV3, AV4). Vibrational couplings were visualized between the C=C of phenol derivatives and C=O of DMF. Interestingly, our experimental observations aligned with the videos for DFT calculations. In AV1 and AV2, the symmetric and asymmetric C=C modes of PC were coupled significantly with amide 1 of DMF; for PCP, the symmetric C=C mode was coupled significantly (AV3) but the asymmetric mode was not (AV4). PC and PCP are phenol derivatives and form hydrogen bonds with amide 1 of DMF, but they showed different vibrational coupling. Hence, phenolic substitution altered the pattern of vibrational coupling.

Vibrational coupling is dependent upon the frequency gap of IR absorption, the distance between two vibration modes, and

Table 1 Vibrational frequencies of IR absorption for the C=C mode and the ratio of IR absorption area for the hydrogen-bonded C=C mode and free C=C mode of phenol derivatives. The enhancement factor and transition dipole moment ratio were calculated from the experimental data shown in Fig. 2

Phenol derivatives	Stretching mode	Frequency (cm^{-1})	IR enhancement ratio (R)	Transition dipole moment ratio
PC	Symmetric	1597.5	1.35	1.16
	Asymmetric	1618.5	1.44	1.20
PCP	Symmetric	1694.0	5.97	2.44
	Asymmetric	1606.5	1	1

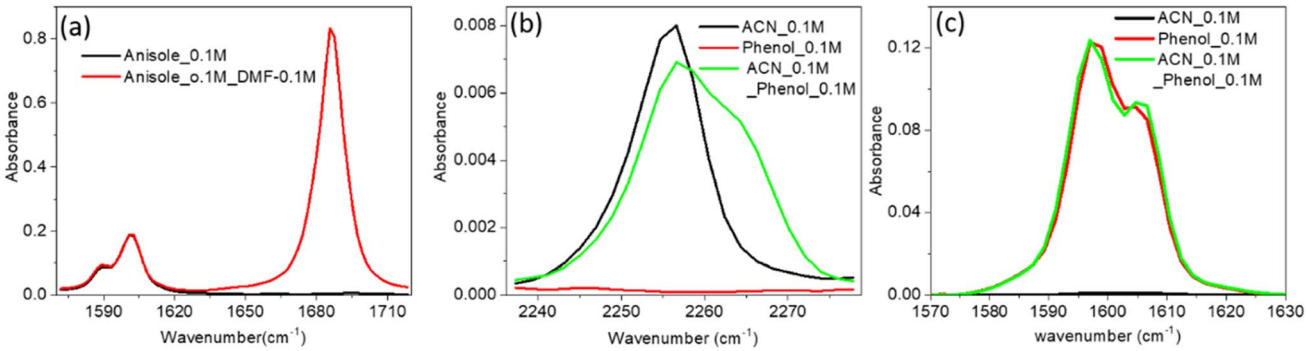

Fig. 3 (a) Linear IR absorbance spectra of the C═C mode of anisole (0.1 M) in the absence (black) and presence (red) of dimethylformamide (0.1 M). (b) IR spectra of the CN mode of ACN (0.1 M) in the absence (black) and presence (green) of phenol (0.1 M) in CCl_4. (c) IR spectra of the C═C mode of phenol (0.1 M) in the absence (black) and presence (red) of ACN (0.1 M).

orientation. The frequency gap between the asymmetric C═C mode of PC and C═O stretching mode of DMF was smaller (56 cm^{-1}) than that of the symmetric C═C and C═O (76 cm^{-1}) modes of PC (Fig. 4a). However, the intensity of asymmetric and symmetric C═C modes was enhanced simultaneously. The frequency gap was smaller for the asymmetric C═C mode (67 cm^{-1}) than symmetric C═C mode (79.5 cm^{-1}) of PCP with amide 1 of DMF. Significant enhancement in IR absorbance was observed for the symmetric C═C mode, but negligible enhancement was observed for the asymmetric C═C mode (Fig. 4b). The distance between the C═C and C═O modes of phenol derivatives and DMF according to DFT calculations are shown in Fig. 4c and d. An identical distance (5.2 Å) between C═C and C═O could not explain the disparity in vibrational coupling. Hence, we assumed that a different transition dipole angle between the C═C mode and amide-I mode was the cause

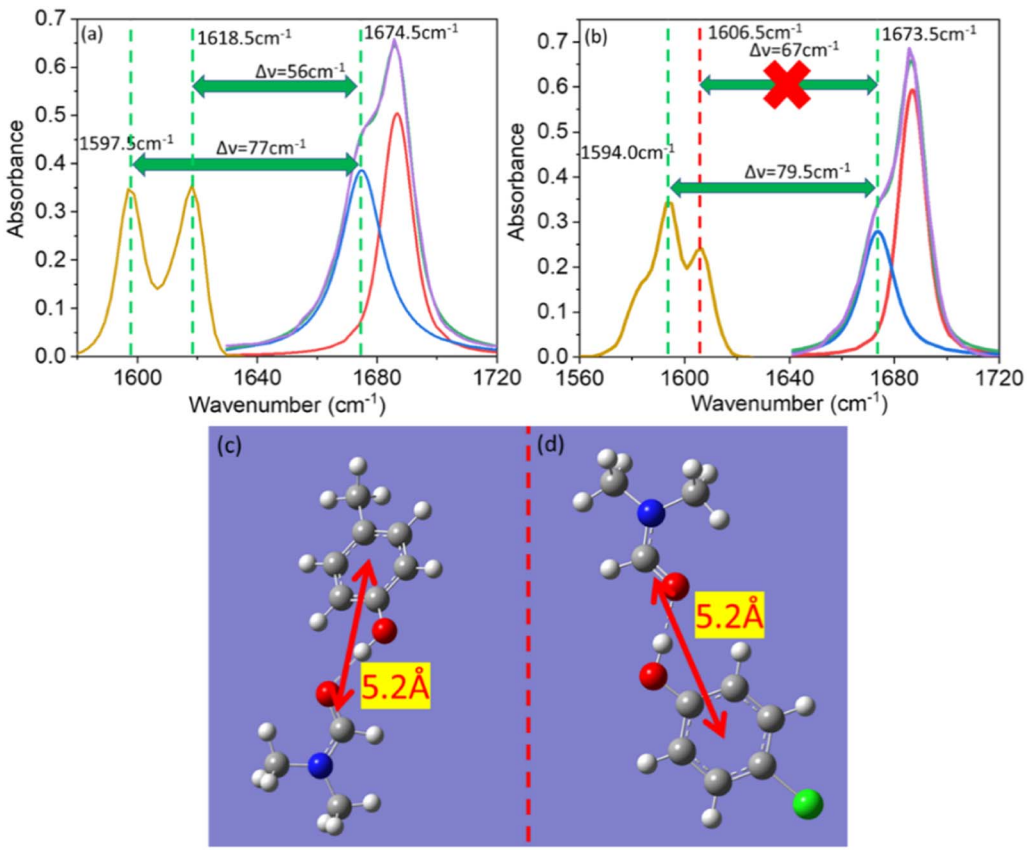

Fig. 4 Linear IR spectra of amide I (dimethylformamide) and the C═C mode of (a) *para*-cresol and (b) *para*-chlorophenol. The IR spectra of amide I (violet), free amide I (red), hydrogen-bonded amide I (blue), cumulative spectra (green), and C═C (gold) are shown. (c) Distance between C═O and C═C of dimethylformamide and *para*-cresol. (d) Distance between C═O and C═C of dimethylformamide and *para*-chlorophenol. A distance of 5.2 Å was calculated (by DFT) for *para*-cresol and *para*-chlorophenol, respectively, with amide I of dimethylformamide.

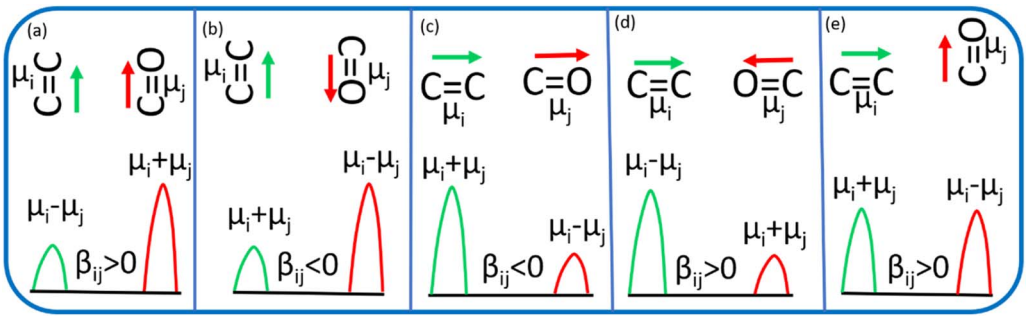

Fig. 5 Red and green denote the linear vibration modes of C=O and C=C, respectively. β_{ij} is the coupling constant, and μ_i, and μ_j are the transition dipole moments of the C=C mode and C=O mode, respectively. Orientation of C=O and C=C modes- (a) parallel (b) antiparallel (c) linearly parallel (d) oppositely parallel and (e) perpendicular.

of this difference in vibrational coupling. To ascertain the reason for this anomalous coupling behaviour, we exposed different orientations between vibration modes (C=C and C=O) (Fig. 5). The sign of the coupling constant (β_{ij}) was dependent upon the geometry of the hydrogen-bonded DMF and phenol derivatives (eqn (1)).[55] If C=C and C=O modes are parallel (Fig. 5a) and β_{ij} is positive, the intensity of the C=O vibrational mode will be enhanced, with a transition dipole moment $\mu_i + \mu_j$. In contrast, the intensity of the C=C vibrational mode will be weaker, with a transition dipole moment $\mu_i - \mu_j$. In the case of antiparallel C=C and C=O modes (Fig. 5b) and negative coupling constant β_{ij}, the C=C mode will be weaker and correspondingly the C=O mode will be stronger, with a transition dipole moment of $\mu_i + \mu_j$ and $\mu_i - \mu_j$, respectively. In the head-to-tail (Fig. 5c) or head-to-head orientation (Fig. 5d) of C=C and C=O, the lower frequency mode of C=C will carry more oscillator strength compared with the C=O mode. An unperturbed intensity will result if the C=C mode and C=O mode are perpendicular to each other (Fig. 5e). The geometries of the DMF–PC complex and DMF–PCP complex are in-between the limits we modelled in Fig. 5. The symmetric and asymmetric C=C modes of PC and symmetric C=C mode of PCP are coupled in the manner shown in Fig. 5c and d. Probably, the asymmetric C=C mode of PCP was coupled with the C=O mode of DMF as shown in Fig. 5e or they were coupled very weakly according to the model shown in Fig. 5a–d.

$$\beta_{ij} = 1/4\pi\varepsilon_0 \left[\frac{\vec{\mu_i} \times \vec{\mu_j}}{r_{ij}^3} - 3 \frac{\left(\vec{r_{ij}} \times \vec{\mu_i}\right)\left(\vec{r_{ij}} \times \vec{\mu_j}\right)}{r_{ij}^5} \right] \quad (1)$$

where β_{ij} is the coupling constant, ε_0 is permittivity, μ_i and μ_j are transition dipole moments, and r_{ij} is the distance between two vibration modes.

We wished to validate our hypotheses of coupling of the symmetric and asymmetric C=C modes of PC and PCP with amide 1. Hence, we carried out DFT calculations of *para*-ethylphenol and *para*-nitrophenol. Surprisingly, we observed the same results as PC for *para*-ethylphenol (AV5, AV6) and as PCP for *para*-nitrophenol (AV7, AV8). We calculated the vibrational coupling for *meta*-chlorophenol and *ortho*-chlorophenol complexes with DMF. The symmetric and asymmetric C=C modes of *meta*-chlorophenol were coupled with amide I (AV9, AV10). The symmetric C=C mode of *ortho*-chlorophenol was coupled with amide I, but the asymmetric C=C mode was not (AV11, AV12). Hence, the C=C symmetric and asymmetric modes coupled with amide 1 for *para*-electron-promoting phenolic compounds. Only the C=C symmetric mode coupled with amide 1 for *para*- and *ortho*-electron-withdrawing-substituted phenolic compounds. The symmetric and asymmetric C=C modes of electron-withdrawing *meta*-substituted phenolic compounds were coupled like *para*-electron-promoting phenolic compounds.

Conclusions

Employment of FTIR spectroscopy and DFT calculations revealed the anomalous vibrational coupling between amide 1 and the C=C mode of phenol derivatives. For PC, IR absorbance was enhanced markedly for symmetric and asymmetric C=C modes upon gradual addition of DMF. For PCP, the symmetric C=C mode was enhanced significantly, whereas the asymmetric C=C mode was not. Even though the frequency gap was less for the asymmetric C=C transition compared with that for the C=O transition, and the distance between C=C and C=O was constant for symmetric and asymmetric C=C modes for PC and PCP, distinctive behaviour was observed for different phenol derivatives in the presence of DMF. Theoretical and experimental observations revealed that, with alteration of phenol substituents, the coupling pattern changed. The area of IR absorbance was enhanced ≈5.97 times for the C=C symmetric mode, whereas it was altered negligibly for the asymmetric mode, in the case of PCP. For PC, the area of IR absorbance for symmetric and asymmetric modes was enhanced significantly (≈1.4 times). Thus, we revealed the nature of vibrational coupling based on the structure of a guest molecule hydrogen-bonded with amide I. Our conclusions could be valuable for depiction of the unusual dynamics of coupled amide-I modes as well as the dependency of vibrational coupling on altered factors.

Conflicts of interest

The authors declare no competing financial interest.

Acknowledgements

AG thanks SNBNCBS, Kolkata, India, for instrumental facilities and financial support from the DST-India. SC thanks DST India for a fellowship.

References

1 R. E. Dickerson and I. Geis, *The Structure and Action of Proteins*, Harper and Row, New York, Evanston, London, 1969.
2 D. L. Nelson and M. M. Cox, *Lehninger Principles of Biochemistry*, W. H. Freeman and Company, New York, 2005.
3 J. M. Berg, J. L. Tymoczko and L. Stryer, *Biochemistry*, W. H. Freeman and Company, New York, 2007.
4 S. Krimm and J. Bandekar, *Adv. Protein Chem.*, 1986, **38**, 181–364.
5 A. Barth and C. Zscherp, *Q. Rev. Biophys.*, 2002, **35**, 369–430.
6 S. Woutersen and P. Hamm, *J. Phys.: Condens. Matter*, 2002, **14**, R1035–R1062.
7 P. Hamm, M. Lim and R. M. Hochstrasser, *J. Phys. Chem. B*, 1998, **102**, 6123–6138.
8 J. Ma, I. M. Pazos, W. Zhang, R. M. Culik and F. Gai, *Annu. Rev. Phys. Chem.*, 2015, **66**, 357–377.
9 R. Adhikary, J. Zimmermann and F. E. Romesberg, *Chem. Rev.*, 2017, **117**, 1927–1969.
10 S. D. Fried and S. G. Boxer, *Acc. Chem. Res.*, 2015, **48**, 998–1006.
11 H. Kim and M. Cho, *Chem. Rev.*, 2013, **113**, 5817–5847.
12 W. Huan, Z. Yanfei, Z. Fengtao, K. Zhengang, H. Buxing, H. Junfeng, W. Zhenpeng and L. Zhimin, *Sci. Adv.*, 2021, **7**(22), 1–9.
13 A. Ghosh, B. Cohn, A. K. Prasad and L. Chuntonov, *J. Chem. Phys.*, 2018, **149**(18), 184501.
14 S. Chakrabarty, A. Barman and A. Ghosh, *J. Phys. Chem. B*, 2022, **126**, 5490–5496.
15 S. Chakrabarty, S. H. Deshmukh, A. Barman, S. Bagchi and A. Ghosh, *J. Phys. Chem. B*, 2022, **126**, 4501–4508.
16 M. K. Gilson and H. X. Zhou, *Annu. Rev. Biophys. Biomol. Struct.*, 2007, **36**, 21–42.
17 R. U. Lemieux, *Acc. Chem. Res.*, 1996, **29**, 373–380.
18 Y. Levy and J. N. Onuchic, *Annu. Rev. Biophys. Biomol. Struct.*, 2006, **35**, 389–415.
19 D. L. Mobley, E. Dumont, J. D. Chodera and K. A. Dill, *J. Phys. Chem. B*, 2007, **111**, 2242–2254.
20 T. H. Plumridge and R. D. Waigh, *J. Pharm. Pharmacol.*, 2002, **54**, 1155–1179.
21 N. S. Myshakina, Z. Ahmed and S. A. Asher, *J. Phys. Chem. B*, 2008, **112**(38), 11873–11877.
22 J. Ma, I. M. Pazos, W. Zhang, R. M. Culik and F. Gai, *Annu. Rev. Phys. Chem.*, 2015, **66**, 357–377.
23 R. Adhikary, J. Zimmermann and F. E. Romesberg, *Chem. Rev.*, 2017, **117**, 1927–1969.
24 S. D. Fried and S. G. Boxer, *Acc. Chem. Res.*, 2015, **48**, 998–1006.
25 H. Kim and M. Cho, *Chem. Rev.*, 2013, **113**, 5817–5847.
26 A. I. Ahmed and F. Gai, *Protein Sci.*, 2017, **26**(2), 375–381.
27 S. Chakrabarty, S. Maity, D. Yazhini and A. Ghosh, *Langmuir*, 2020, **36**, 11255–11261.
28 A. Ghosh, A. K. Prasad and L. Chuntonov, *J. Phys. Chem. Lett.*, 2019, **10**, 2481–2486.
29 D. G. Brown and J. Bostrom, *J. Med. Chem.*, 2016, **59**, 4443–4458.
30 V. R. Pattabiraman and J. W. Bode, *Nature*, 2011, **480**, 471–479.
31 A. B. Hughes, Origins and Synthesis of Amino Acids, *Amino Acids, Peptides and Proteins in Organic Chemistry*, Wiley-VCH, Weinheim, Germany, 2009, vol. 1.
32 A. A. Kaspar and J. M. Reichert, *Drug Discovery Today*, 2013, **18**, 807–817.
33 R. B. Dyer, F. Gai, W. H. Woodruff, R. Gilmanshin and R. H. Callender, *Acc. Chem. Res.*, 1998, **31**, 709–716.
34 S. Woutersen, R. Pfister, P. Hamm, Y. Mu, D. S. Kosov and G. Stock, *J. Chem. Phys.*, 2002, **117**, 6833–6840.
35 N. Demirdöven, C. M. Cheatum, H. S. Chung, M. Khalil, J. Knoester and A. Tokmakoff, *J. Am. Chem. Soc.*, 2004, **126**, 7981–7990.
36 M. M. Waegele, R. M. Culik and F. Gai, *J. Phys. Chem. Lett.*, 2011, **2**, 2598–2609.
37 A. L. Serrano, M. M. Waegele and F. Gai, *Protein Sci.*, 2012, **21**, 157–170.
38 H. Kim and M. Cho, *Chem. Rev.*, 2013, **113**(8), 5817–5847.
39 P. Hamm, and R. M. Hochstrasser, *Ultrafast Infrared, and Raman Spectroscopy*, 2001.
40 A. M. Cunha, E. Salamatova, R. Bloem, S. J. Roeters, S. Woutersen, M. S. Pshenichnikov and T. L. C. Jansen, *J. Phys. Chem. Lett.*, 2017, **8**, 2438–2444.
41 H. Li, R. Lantz and D. Du, *Molecules*, 2019, **24**, 186.
42 W. M. Zhang, V. Chernyak and S. Mukamel, *J. Chem. Phys.*, 1999, **110**, 5011–5028.
43 C. Scheurer, A. Piryatinski and S. Mukamel, *J. Am. Chem. Soc.*, 2001, **123**, 3114–3124.
44 A. Moran and S. Mukamel, *Proc. Natl. Acad. Sci. U. S. A.*, 2004, **101**, 506–510.
45 E. G. Buchanan, W. H. James, S. H. Choi, L. Guo, S. H. Gellman, C. W. Müller and T. S. Zwier, *J. Chem. Phys.*, 2012, **137**, 094301.
46 M. Lima, R. Chelli, V. V. Volkov and R. Righini, *J. Chem. Phys.*, 2009, **130**, 204518.
47 S. Krimm and Y. Abe, *Proc. Natl. Acad. Sci. U. S. A.*, 1972, **69**, 2788–2792.
48 S. Roy, T. L. C. Jansen and J. Knoester, *Phys. Chem. Chem. Phys.*, 2010, **12**, 9347–9357.
49 C. Liang, M. Louhivuori, S. J. Marrink, T. L. C. Jansen and J. Knoester, *J. Phys. Chem. Lett.*, 2013, **4**, 448–452.
50 J. Schaefer, H. G. Ellen, Y. N. Backus and M. Bonn, *J. Phys. Chem. Lett.*, 2016, **7**, 4591–4595.
51 I. V. Rubtsov, J. Wang and R. M. Hochstrasser, *J. Phys. Chem. A*, 2003, **107**, 3384–3396.
52 J. V. Hatton and R. E. Richards, *Mol. Phys.*, 1960, **3**, 253–263.
53 M. Malathi, R. Sabesan and S. Krishnan, *Curr. Sci.*, 2002, **86**, 838–842.
54 A. Ghosh, *J. Phys. Chem. B*, 2019, **123**, 7771–7776.
55 P. Hamm and M. Zanni, *Concepts and Methods of 2D Infrared Spectroscopy*, Cambridge University Press, New York, 2011.